2021 43rd Annual International Conference of the
IEEE Engineering in Medicine & Biology Society (EMBC)
Oct 31 - Nov 4, 2021. Virtual Conference

Shear Wave Speed estimator using Continuous Wavelet Transform for Crawling Wave Sonoelastography

Sebastian Merino[1], Stefano E. Romero [1], Eduardo A. Gonzalez [2] and Benjamin Castaneda[1]

***Abstract*— Crawling Wave Sonoelastography (CWS) is an elastography ultrasound-based imaging approach that provides tissue stiffness information through the calculation of Shear Wave Speed (SWS). Many SWS estimators have been developed; however, they report important limitations such as the presence of artifacts, border effects or high computational cost. In addition, these techniques require a moving interference pattern which could be challenging for *in vivo* applications. In this study, a new estimator based on the Continuous Wavelet Transform (CWT) is proposed. This allows the generation of a SWS image for every sonoelasticity video frame. Testing was made with data acquired from experiments conducted on a gelatin phantom with a circular inclusion. It was excited with two vibration sources placed at both sides with frequencies ranging from 200 Hz to 360 Hz in steps of 20 Hz. Results show small variation of the SWS image across time. Additionally, images were compared with the Phase Derivative method (PD) and the Regularized Wavelength Average Velocity Estimator (R-WAVE). Similar SWS values were obtained for the three estimators within a certain region of interest in the inclusion (At 360 Hz, CWT: 5.01±0.2m/s, PD: 5.11±0.28m/s, R-WAVE: 4.51±0.62m/s) and in the background (At 360 Hz, CWT: 3.67±0.15m/s, PD: 3.69±0.23m/s, R-WAVE: 3.58±0.24m/s). CWT also presented the lowest coefficient of variation and the highest contrast-to-noise ratio for most frequencies, which allows better discrimination between regions.**

***Clinical relevance*— This study presents a new Shear Wave Speed estimator for Crawling Wave Sonoelastography, which can be useful to characterize soft tissue and detect lesions.**

I. Introduction

Quantitative ultrasound elastography has been widely used over the last thirty years to obtain information of the stiffness for the characterization of soft tissues (*e.g.*, muscle [1], diabetic foot [2], liver [3]) as well as the detection of hard lesions such as prostate tumors [4] [5]. This approach is based on the tracking of shear waves in order to estimate the Shear Wave Speed (SWS), since it is directly related to tissue stiffness by the Young's module. In that sense, Crawling Wave Sonoelastography (CWS), is based on a slowly moving interference pattern produced by two external sources vibrating at slightly different frequencies. This allows the acquisition of a SWS distribution map of the tissue [6] which has statistically reliable results compared to mechanical measurements and other elastography techniques [7].

In CWS, multiple methods have been developed to reconstruct a SWS map given the tissue displacement. An initial technique based on a cross-correlation approach proposed in [8] uses the relationship between the spatial phase derivative and local SWS. Subsequently, Hah *et al.* proposed the Phase Derivative (PD) approach which is an alternative based on taking the derivative along the slow time dimension [9]. Even though both approaches have been tested, the report of high variance due to artifacts in the background is still a limitation on the SWS map. In addition, another method called the Regularized Wavelength Average Velocity Estimator (R-WAVE) was proposed [10]. This estimator is based on the average of the spatial wavelength of the signal. It also implements a regularization method to cope with underestimation. Despite exhibiting overall better performance than PD and the cross-correlation approach, this last technique also presents a high execution time. For these reasons, there is constant research towards developing new algorithms for SWS estimation.

In this paper, a new estimator based on the Continuous Wavelet Transform (CWT) is proposed. This transform uses functions called wavelets to measure the presence of local frequencies in the signal. For this reason, local spatial frequency of the interference signal can be found and, consequently, the SWS in a given region can be calculated. Effectiveness of this new method will be assessed in data collected from experiments in a gelatin phantom with a stiffer inclusion at several frequencies. In addition, the results will be compared with PD and R-WAVE estimators.

II. Theory

A. Crawling Waves Sonoelastography

In the usual setup proposed by Wu *et al.* [11], two mechanical sources with frequencies f and $f+\Delta f$ are placed at the sides of a tissue generating a displacement pattern due to the superposition of both signals. This effect is described by equation 1.

$$|u(x,t)|^2 = 2e^{-\alpha_c D} cos[(2k+\Delta k)x + \Delta w t] \qquad (1)$$

where α_C is the attenuation of the medium, D is the distance between sources, k represents the wave number and $\Delta w = 2\pi\Delta f$. Also, the shear wave speed is given by

$$c_s = \frac{w}{k} = \frac{f}{\xi} \qquad (2)$$

*Benjamin Castaneda was supported by the PUCP Research Period Award.

[1]S. Merino, S. Romero and B. Castaneda are with Laboratorio de Imagenes Medicas, Departamento de Ingeniería, Pontificia Universidad Catolica del Perú, Avenida Universitaria 1801, Lima, Perú. sebastian.merino@pucp.edu.pe, castaneda.b@pucp.edu.pe, sromerog@pucp.pe

[2]E. Gonzalez is with Johns Hopkins University, Maryland, USA egonza31@jhmi.edu

where $\xi = k/2\pi$ is the spatial frequency of the original signal. It is noted that the interference spatial frequency ξ', from (1) becomes approximately twice the true spatial frequency:

$$\xi' = \frac{2k + \Delta k}{2\pi} \approx \frac{2k}{2\pi} = 2\xi \tag{3}$$

Therefore, we can relate ξ' to the shear wave speed with the equation:

$$c_s = \frac{2f}{\xi'} \tag{4}$$

B. Continuous Wavelet Transform

In wavelet theory, the Continuous Wavelet Transform (CWT) measures the similarity of a signal with basis functions called wavelets, which are scaled or translated versions from a function called the mother wavelet. It is defined by the following:

$$W(a,b) = \frac{1}{\sqrt{a}} \int_{-\infty}^{\infty} \psi^* \left(\frac{x-b}{a} \right) f(x) dx \tag{5}$$

Where $\psi(x)$ is the mother wavelet, and a and b are the scaling and translation parameters, respectively. The first one determines the frequency of the scaled wavelet, and the second one determines its position.

In the proposed estimator, a Morse wavelet was chosen as the mother wavelet. The Fourier transform of the Morse wavelet family is defined by:

$$\Psi(\omega) = a_{P,\gamma} U(\omega) e^{-\omega^\gamma} \omega^{P^2/\gamma} \tag{6}$$

Where $a_{P,\gamma}$ is the normalization constant, $U(\omega)$ is the unit step function, P^2 is the time-bandwidth product and γ is a parameter that characterizes the symmetry of the wavelet. The value of γ was set to 3, as it generates the most symmetric wavelet of the Morse family [12], and P^2 was set to 4, as low values enhance spatial resolution.

The CWT is computed across the lateral dimension for each frame and each depth slice of the sonoelasticity video, as shown in Figure 1. Then, the value of a that gives the maximum value of the Wavelet transform for every x coordinate is found. The local spatial frequency of the signal would become $1/a$ times the frequency of the mother wavelet. Hence, using Eq. (4) a SWS map can be generated for each frame.

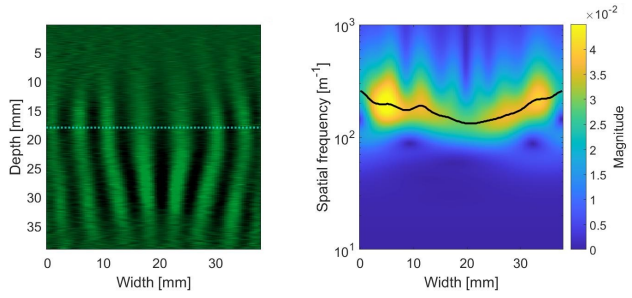

Fig. 1: (a) Sonoelasticity video frame at 360 Hz. The CWT is computed across the lateral dimension for each depth slice. (b) CWT magnitude scalogram for 18 mm depth. The maximum values for each x coordinate are calculated and marked as a black line.

III. Materials and Methods

A. Experimental setup

The data was acquired from experiments conducted in the framework of Romero *et al* [13]. A gelatin phantom of 13 cm x 13 cm x 9 cm with a 15.5 mm-diameter cylinder inclusion at 10 mm from the top was elaborated for testing. The ground truth SWS values were obtained using the time of flight (TOF) test, resulting in 3.45 m/s for the background and 5.1 m/s for the inclusion. The same setup used in [11], with two vibrating parallel plates attached to the lateral sides of the phantom, was used for frequencies ranging from 200 Hz to 360 Hz in 20 Hz steps. Color radio frequency data was acquired from an ultrasound probe from a SonixTOUCH Research System using a L14-5/38 linear array operating at 6.6 MHz at a depth of 4 cm. A sonoelasticity video was obtained using Miller's spectral moment estimator [14].

B. Pre-processing

The data was further processed using a 2D median filter with a 0.87 mm x 0.89 mm window for each frame and then normalized, eliminating the DC component. Moreover, a directional gaussian filter on the two-dimensional Fourier transform was applied to filter frequencies outside the usual SWS range (2 m/s - 7 m/s).

C. Metrics

A SWS map was computed using the CWT for each sonoelasticity frame. The coefficient of variation (CV) of each frame was calculated. In addition, a selected region of interest (ROI) in the inclusion of 11 x 11mm and two on the background of 5.5 x 11mm were selected to measure both parts of the phantom for each estimator. The mean value, standard deviation, bias, CV and Contrast-to-Noise Ratio (CNR) were evaluated to compare the results. This last metric is defined by the following equation:

$$CNR = 20 \log_{10} \left(\frac{2\left(\mu_1 - \mu_2\right)^2}{\sigma_1^2 + \sigma_2^2} \right) \tag{7}$$

where μ_1 and μ_1 are the mean of the SWS, and σ_1 and σ_2 are the standard deviation inside and outside the inclusion, respectively.

IV. Results

Figure 2 (a) shows a representative result of the SWS estimation for each frame using the CWT algorithm, as well as Figure 2 (b) shows a CV map for each pixel. As it can be appreciated, low values in each pixels were typically found, especially at the center of the image, where the CV is usually less than 2%. Then, for comparison purposes, a single SWS image was generated by using the mean value of each pixel across time.

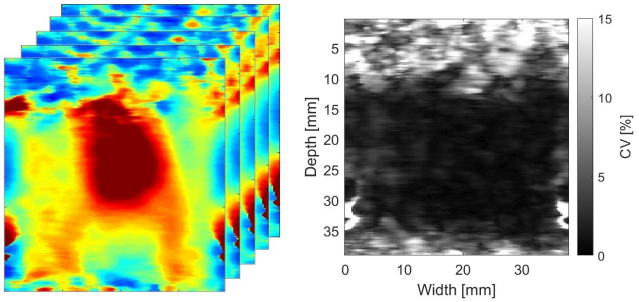

(a) (b)

Fig. 2: (a) Shear Wave Speed for each sonoelasticity crawling wave frame at 360 Hz. (b) Coefficient of Variation in each pixel of the Shear Wave Speed Map.

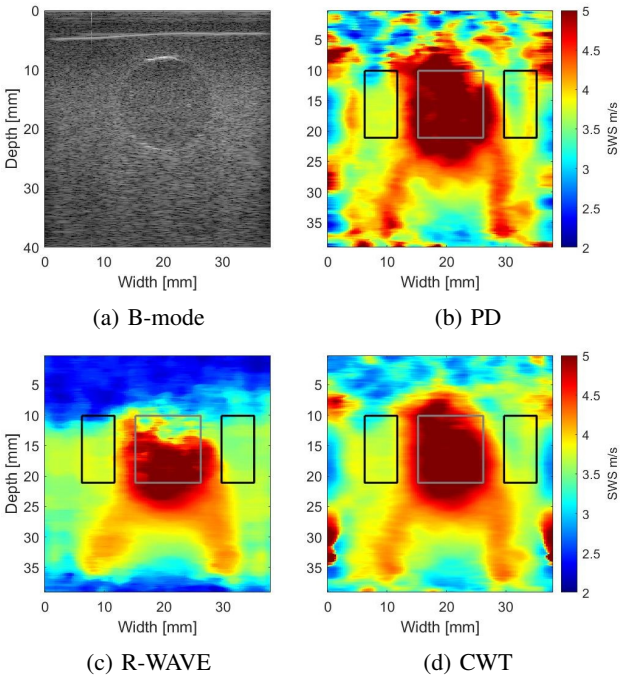

(a) B-mode (b) PD

(c) R-WAVE (d) CWT

Fig. 3: Images obtained at 360 Hz with various SWS estimators.

Afterwards, SWS images at several frequencies were obtained using the three estimators. For R-WAVE, the regularization parameter α was set to 1.2. Results for 360 Hz are shown in Figure 3. The mean SWS for the inclusion was $5.01 \pm 0.2m/s$ for CWT, $5.11 \pm 0.28m/s$ for PD and $4.51 \pm 0.62m/s$ for R-WAVE. PD and CWT showed better performance in the inclusion compared to R-WAVE, due to high underestimation in the upper border. In the background region, the mean SWS was $3.67 \pm 0.15m/s$ for CWT, $3.69 \pm 0.23m/s$ for PD and $3.58 \pm 0.24m/s$ for R-WAVE. CWT presented less variability in both regions, with a CV of 3.94% in the inclusion and 4.01% in the background.

Figure 4 shows summarized data for several frequencies. Similar performances for SWS mean in the three estimators are observed with overestimation in the background region. In the inclusion, most images show low bias (less than 5%), yet R-WAVE appears to have abnormally high bias (more than 10%) for frequencies ranging from 320 to 360 Hz due to underestimation. In the background, PD has the higher bias for frequencies above 280 Hz, and CWT appears to have better performance for low frequencies (below 260 Hz). Additionally, CWT exhibits the lower CV in the inclusion for almost all frequencies. For the background region, this occurs in frequencies higher than 280 Hz.

Similarly, CNR at different frequencies is shown in Figure 5. For most of them, CWT presents higher CNR values, and overall it presents a higher average (PD: 25.52 dB, R-WAVE: 19.83 dB, CWT: 30.18 dB). In addition, CNR seems to improve with higher frequencies, considering that the highest value (35.5 dB) was obtained at 360 Hz.

V. Discussion

The CWT estimator successfully generated a SWS image in a heterogeneous phantom. Firstly, considering that this approach generates a SWS map for every sonoelasticity frame, results demonstrate that it is independent of the interference pattern movement. The CV across time show small variation between frames, especially below 10 mm depth, as shown in 2. This represents an advantage in contrast to other estimators, such as PD, which requires time information about the interference pattern. In addition to this, because regions with artifacts present higher CV, it can also serve as a quality measure.

Additionally, the metrics in 4 show that, like in the PD method, low bias in the inclusion (less than 6.5%) is obtained. CWT also provided a more stable image in most frequencies, according to his CV inside the ROI. For this reason, CWT provides high CNR compared to the other two estimators, especially in higher frequencies (340 - 360 Hz), as shown in 5. This allows better discrimination between regions and is another advantage of this method.

While R-WAVE provides more accurate estimation in the background region, high underestimation in the inclusion is observed in images from higher frequencies (320 - 360 Hz), like the one shown in 3(c). However, CWT and PD seem to generate a better image. A possible reason for this is that frequency analysis might be more effective to obtain instantaneous frequencies in a noisy signal than the space-domain analysis performed in R-WAVE.

Finally, the proposed estimator also has some limitations, such as artifacts at the border. This effects are common when using the CWT because stretched wavelets extend beyond the edges of the signal, therefore, to compute the algorithm, the signal must be expanded. In this paper, each sonoelasticity video frame was extended periodically along the horizontal axis to obtain a stable SWS video. Consequently, higher SWS values are found at the border, which might be misleading and indicate the presence of non-existent stiffer regions. Nevertheless, results at the center of the image give an accurate estimation of SWS and show overall better performance than previously developed estimators.

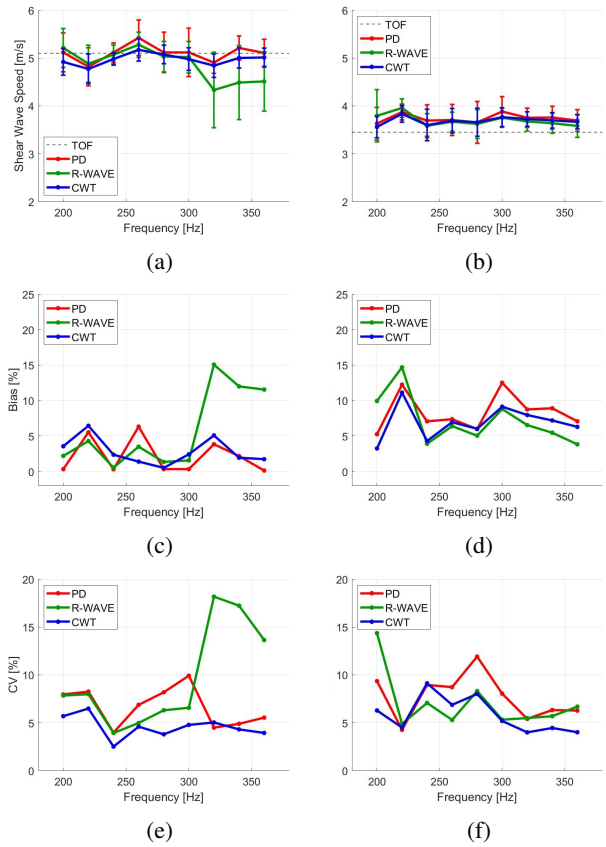

Fig. 4: SWS [m/s] mean of ROI of (a) Inclusion (b) Background. Bias[%] for (c) Inclusion (d) Background. CV[%] for (e) Inclusion (f) Background.

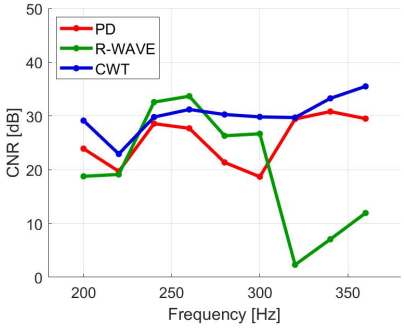

Fig. 5: CNR among different frequencies.

VI. Conclusions and Future Work

A new shear wave speed estimator for CWS based on the CWT was proposed. Preliminary results on heterogeneous phantoms show that the algorithm provides a stable SWS video and has high accuracy in comparison to other estimators such as PD and R-WAVE. It also has a higher CNR, which allows better discrimination of abnormal regions. However, the image seems to have irregular borders, which may affect accuracy and lead to false positives. Future work might include optimization to improve execution time and develop real-time applications, signal extension techniques to address artifacts at the border and applications of the algorithm with other experimental setups such as normal excitation.

VII. Acknowledgements

The authors thank BSc Valeria León for their helpful suggestions and support.

References

[1] E. A. Gonzalez, S. E. Romero, and B. Castaneda, "Real-time crawling wave sonoelastography for human muscle characterization: Initial results," *IEEE transactions on ultrasonics, ferroelectrics, and frequency control*, vol. 66, no. 3, pp. 563–571, 2018.

[2] R. Naemi, S. E. Romero Gutierrez, D. Allan, G. Flores, J. Ormaechea, E. Gutierrez, J. Casado-Pena, S. Anyosa-Zavaleta, M. Juarez, F. Casado *et al.*, "Diabetes status is associated with plantar soft tissue stiffness measured using ultrasound reverberant shear wave elastography approach," *Journal of Diabetes Science and Technology*, p. 1932296820965259, 2020.

[3] J. Ormachea, K. J. Parker, and R. G. Barr, "An initial study of complete 2d shear wave dispersion images using a reverberant shear wave field," *Physics in Medicine & Biology*, vol. 64, no. 14, p. 145009, 2019.

[4] K. Parker, S. Huang, R. Musulin, and R. Lerner, "Tissue response to mechanical vibrations for "sonoelasticity imaging"," *Ultrasound in medicine & biology*, vol. 16, no. 3, pp. 241–246, 1990.

[5] B. Castaneda, L. An, S. Wu, L. L. Baxter, J. L. Yao, J. V. Joseph, K. Hoyt, J. Strang, D. J. Rubens, and K. J. Parker, "Prostate cancer detection using crawling wave sonoelastography," in *Medical Imaging 2009: Ultrasonic Imaging and Signal Processing*, vol. 7265. International Society for Optics and Photonics, 2009, p. 726513.

[6] Z. Wu, K. Hoyt, D. J. Rubens, and K. Parker, "Sonoelastographic imaging of interference patterns for estimation of shear velocity distribution in biomaterials," *Journal of the Acoustical Society of America*, vol. 120, no. 1, pp. 535–545, April 2006.

[7] J. Ormachea, R. J. Lavarello, S. A. McAleavey, K. J. Parker, and B. Castaneda, "Shear wave speed measurements using crawling wave sonoelastography and single tracking location shear wave elasticity imaging for tissue characterization," *IEEE transactions on ultrasonics, ferroelectrics, and frequency control*, vol. 63, no. 9, pp. 1351–1360, 2016.

[8] K. Hoyt, K. J. Parker, and D. J. Rubens, "Real-time shear velocity imaging using sonoelastographic techniques," *Ultrasound in medicine & biology*, vol. 33, no. 7, pp. 1086–1097, 2007.

[9] Z. Hah, C. Hazard, B. Mills, C. Barry, D. Rubens, and K. Parker, "Integration of crawling waves in an ultrasound imaging system. part 2: signal processing and applications," *Ultrasound in medicine & biology*, vol. 38, no. 2, pp. 312–323, 2012.

[10] E. González, P. Li, J. Ormachea, K. Parker, R. Lavarello, and B. Castañeda, "Regularized wavelength average velocity estimator for quantitative ultrasound elastography," in *2016 IEEE International Ultrasonics Symposium (IUS)*. IEEE, 2016, pp. 1–4.

[11] Z. Wu, L. Taylor, D. J. Rubens, and K. Parker, "Sonoelastographic imaging of interference patterns for estimation of the shear velocity of homogeneous biomaterials," *Physics in medicine and biology*, vol. 49, no. 6, pp. 911–922, March 2004.

[12] J. M. Lilly and S. C. Olhede, "Generalized morse wavelets as a superfamily of analytic wavelets," *IEEE Transactions on Signal Processing*, vol. 60, no. 11, pp. 6036–6041, 2012.

[13] S. E. Romero, E. A. Gonzalez, R. Lavarello, and B. Castañeda, "A comparative study between parallel and normal excitation for crawling wave sonoelastography," in *12th International Symposium on Medical Information Processing and Analysis*, vol. 10160. International Society for Optics and Photonics, 2017, p. 101601G.

[14] K. Miller and M. Rochwarger, "A covariance approach to spectral moment estimation," *IEEE Transactions on Information Theory*, vol. 18, no. 5, pp. 588–596, 1972.